ACS OMEGA

http://pubs.acs.org/journal/acsodf

Article

Quantum-Mechanical Driven ^{1}H Iterative Full Spin Analysis Addresses Complex Peak Patterns of Choline Sulfate

Yun-Seo Kil and Joo-Won Nam*

Cite This: *ACS Omega* 2022, 7, 42607−42612

Read Online

ACCESS | Metrics & More | Article Recommendations | Supporting Information

ABSTRACT: Choline and choline esters are essential nutrients in biological systems for carrying out normal functions, such as the modulation of neurotransmission and the formation and maintenance of cell membranes. Choline sulfate is reportedly involved in the defense mechanism of accumulating sulfur resources against sulfur deficiency. Contrary to expectations, a full assignment of the ^{1}H NMR spectrum of choline sulfate has not been reported. The present study pioneered a full assignment by quantum-mechanical driven ^{1}H iterative full spin analysis. The complex peak patterns were analyzed in terms of heteronuclear and non-first-order coupling. The ^{1}H−^{14}N coupling constants, including two-bond coupling, which can be neglected, were accurately determined by iterative optimization. Non-first-order splitting has been described to be due to the presence of magnetically non-equivalent geminal protons. Moreover, in the comparison of the methylene proton resonance patterns of choline sulfate with choline and choline phosphate, the differences in the geminal and vicinal coupling constants were further examined through spectral simulation excluding the heteronuclear coupling. The precise spectral interpretation provided in this study is expected to contribute to future ^{1}H NMR-based qualitative or quantitative studies of choline sulfate-containing sources.

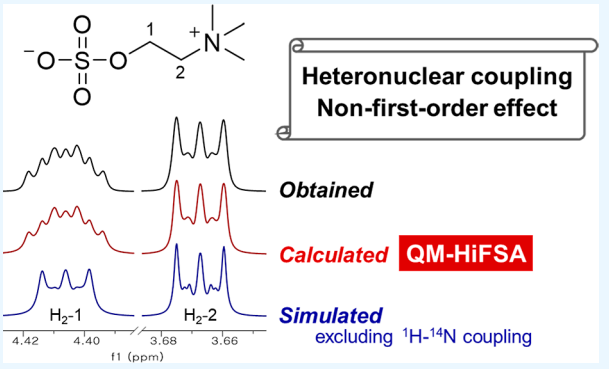

1. INTRODUCTION

Choline and choline esters are essential for the normal functioning of biological systems. Choline is a biosynthetic precursor of choline esters including acetylcholine, choline phosphate (phosphocholine), glycerophosphocholine, phosphatidylcholine, and sphingomyelin. Acetylcholine is a crucial chemical messenger at the synapses in the nervous system. Phosphatidylcholine and sphingomyelin are the major components of biological membranes.[1] In our previous ^{1}H NMR-based metabolomics study, a sulfate ester of choline (i.e., choline sulfate) was observed in wheat bran extract samples, along with betaine and choline.[2] Choline sulfate in plants aids in the defense mechanism against sulfur deficiency by accumulating sulfur resources.[3,4] Choline sulfate has also been reported as a fungal[5] and bacterial metabolite,[6] possibly related to the presence of choline sulfate in host plants.

The effective use of the structural and quantitative information contained in NMR spectra requires an elaborate interpretation of the spectral information, including chemical shifts (δ) and coupling constants (J). Quantum-mechanical driven ^{1}H iterative full spin analysis (QM-HiFSA) increases the accuracy of the interpretation of spectral information over conventional manual spectral analysis. QM-HiFSA advances metabolomic standardization by establishing complete δ/J profiles and thus achieving more accurate quantification results. The detection of pure first-order spin systems in relatively rare cases has further led to the application of the quantum-mechanical driven iterative analysis in chemical standardization.[7−11]

The present study aims to address the absence of a complete assignment of the ^{1}H NMR spectrum of choline sulfate. In the context of the need for a compound information library of choline sulfate for qualitative or quantitative studies, our previous ^{1}H NMR-based metabolomics study provided a full set of 1D and 2D NMR spectra of choline sulfate, along with a custom ChemAdder library file.[2] However, the complete ^{1}H NMR signal assignment of choline sulfate remains a challenge because of the presence of ^{1}H−^{14}N heteronuclear and non-first-order (i.e., higher-order) coupling. In the present study, QM-HiFSA was strategically used for the complete analysis of complex peak patterns of choline sulfate. This study entailed effective descriptions of the phenomena and quantum-mechanical driven spectral calculations accompanied by standardized NMR terms, including the resonance, signal, pattern, peak, line, transition, splitting, multiplicity, resolution, and dispersion.[12] Moreover, accurate δ and J values resulting from

Received: September 21, 2022
Accepted: November 2, 2022
Published: November 10, 2022

QM-HiFSA were provided at levels of 0.1 ppb and 10 mHz, respectively, as previously recommended.[13]

2. EXPERIMENTAL SECTION

2.1. Chemicals and Instrumentation. Choline sulfate (98%) was purchased from Cambridge Isotope Laboratories (Tewksbury, MA, USA). Choline chloride (>98%) and phosphocholine chloride calcium salt tetrahydrate (>98%) were obtained from TCI Chemicals (Tokyo, Japan). NMR samples of standard compounds were each prepared at a concentration of 10 mM in D_2O, respectively. ^{1}H NMR spectra were acquired on a Bruker AVANCE NEO spectrometer (^{1}H, 600 MHz, Oxford magnet, Bruker Switzerland AG, Fällanden, Switzerland), operated using Bruker TopSpin 4.1.3 software (Billerica, MA, USA), at the Core Research Support Center for Natural Products and Medical Materials (CRCNM).

^{1}H NMR spectra of the standard compounds (choline sulfate, choline, and choline phosphate) were acquired using a 1D NOESY presat pulse sequence (noesypr1d, TopSpin, Bruker) with a probe temperature at 298 K, a calibrated 90° pulse, a relaxation delay of 2 s, an acquisition time of 4 s, a spectral width of 16 ppm (centered at 4.70 ppm), a receiver gain of 64, the number of scans of 32, and the number of dummy scans of 2. Post-acquisition processing, including third-order polynomial fitting for baseline correction, manual phasing, and a line broadening of 0.3, was conducted using the MestReNova 12.0.3 software (Mestrelab Research SL, Santiago de Compostela, Spain).

2.2. Computational Analysis. The spectral calculation (i.e., QM-HiFSA) and simulation were performed using ChemAdder 0.8.7 software, as previously described.[11,14]

The calculation process comprised three major steps: (i) creating spin systems by executing ^{1}H NMR predictions on an imported 3D chemical structure, (ii) manually editing chemical shifts by matching the corresponding patterns in the experimental spectrum, and (iii) iteratively adjusting and optimizing the calculated ^{1}H NMR parameters using the least-squares fitting method "total-line shape fitting" or "auto-fit." Further optimization could be achieved by changing the line width optimization modes ["force to original" (default) to "release"] and adjusting the Gaussian, asymmetry, or dispersion contributions. The total root-mean-square (RMS) value indicates the degree of similarity between the calculated and experimental spectra.

The spectral simulation was performed to exclude heteronuclear coupling for highlighting the phenomenon observed in the line shapes of choline sulfate compared to those of choline and choline phosphate. The simulation process accordingly excluded the heteronuclear coupling values from the parameters obtained from the preceding calculation. Subsequently, to generate an NMR spectrum for the given parameters, the "simulate" function was executed.

3. RESULTS AND DISCUSSION

The present study for the first time established the QM-HiFSA profile of choline sulfate (Table 1 and Figure S1 and S2 in the Supporting Information). This report describes the complex peak patterns of choline sulfate considering two aspects: heteronuclear and non-first-order coupling. Choline and choline phosphate were also subjected to the QM-HiFSA process (S3 for choline and S4 for choline phosphate in the Supporting Information) for comparative interpretation. The QM-HiFSA profile of choline in this study was in good agreement with a recent computational study of the ^{1}H NMR spectrum of choline.[15] The full spin analysis of choline phosphate yielded chemical shift and coupling constant values comparable to that from a previous spectral optimization and simulation,[16] but significant progress was made in the present study, involving small ^{1}H−^{14}N and ^{1}H−^{31}P couplings. Moreover, the present analysis provides a systematic understanding of the non-first-order coupling rather than reporting only separate J values as before.

Table 1. QM-HiFSA Profiles of Choline Sulfate, Choline, and Choline Phosphate[a]

	δ_H (in ppm) {J in Hz}		
position	choline sulfate	choline	choline phosphate
1	4.4060	3.9694	4.0692
	{−13.81*, 7.16, 2.12, 2.66(N)}	{−13.80*, 6.89, 3.16, 2.69(N)}	{−13.70*, 6.98, 2.54, 2.78(N), 5.61(P)}
2	3.6673	3.4261	3.4969
	{−14.78*, 7.16, 2.12, 0.37(N)}	{−13.78*, 6.89, 3.16, 0.33(N)}	{−13.61*, 6.98, 2.54, 0.39(N), 0.71(P)}
NCH_3	3.1377	3.1089	3.1254
	{0.48(N)}	{0.54(N)}	{0.57(N)}

[a]The spectral calculation was performed using ^{1}H NMR spectra acquired in D_2O at 600 MHz with the 1D NOESY presat pulse sequence (noesypr1d; water signal suppression with δ_H 4.70 ppm of a presaturation frequency). Asterisks (*) denote geminal coupling ^2J. ^{1}H−^{14}N and ^{1}H−^{31}P coupling constants are indicated in brackets {()} by N and P, respectively.

3.1. Heteronuclear Coupling. A nitrogen nucleus (^{14}N) with a spin quantum number of 1 has a moderate-sized nuclear quadrupole moment. Thus, when the ^{14}N nucleus is placed in a highly symmetrical environment (such as in tetraalkylammonium salts), it has a small quadrupole moment, which slows nuclear transitions and results in resolvable coupling.[17] Consequently, the interpretation of heteronuclear coupling of choline nitrogen (^{1}H− or ^{13}C−^{14}N coupling) is important for the complete assignment of the ^{1}H or ^{13}C NMR spectra of choline and choline esters. The ^{13}C−^{14}N coupling has been fully disclosed, reporting substantial J values ($^1J_{CN}$, 3−4 Hz); C-2 and NCH_3 are observed as distinct 1:1:1 triplets in the ^{1}H-decoupled ^{13}C NMR spectrum.[2,17−19] However, the precise determination of ^{1}H−^{14}N coupling, especially in manual spectral analysis, is a challenge because of the small (<1 Hz) two-bond coupling constant ($^2J_{HN}$).[16,20,21]

In the present study, the QM-HiFSA fully examined the ^{1}H−^{14}N heteronuclear coupling of choline sulfate. Three ^{1}H−^{14}N coupling constant values were obtained (Table 1 and Figure 1): 2.66 Hz ($^3J_{HN}$ of the methylene protons at C-1), 0.37 Hz ($^2J_{HN}$ of the methylene protons at C-2), and 0.48 Hz ($^2J_{HN}$ of the N-methyl group protons). Choline and choline phosphate were also found to have comparable ^{1}H−^{14}N coupling constants. Most notably, the two-bond coupling constants with fairly small values were effectively determined (~0.5 Hz).

The full spin analysis of choline phosphate also afforded ^{1}H−^{31}P coupling values, including a four-bond heteronuclear coupling ($^4J_{HP}$) of 0.71 Hz (Table 1 and Figure 1). This is the first study optimizing the small $^4J_{HP}$ of a phosphate ester compound of choline, even though a computational study on the $^4J_{HP}$ of simple ethyl pyrophosphates exists.[22]

3.2. Non-First-Order Coupling. In addition to the heteronuclear coupling, conformational properties of choline

https://doi.org/10.1021/acsomega.2c06092
ACS Omega 2022, 7, 42607−42612

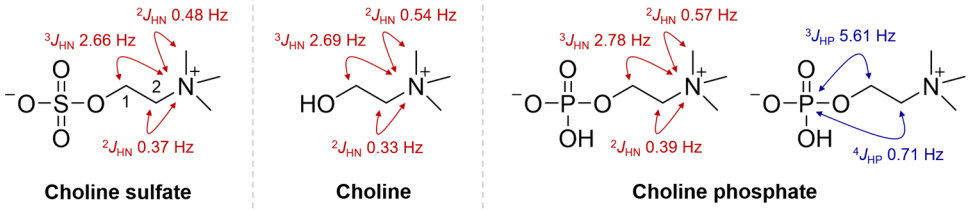

Figure 1. Calculated ^{1}H−^{14}N and ^{1}H−^{31}P couplings of choline sulfate, choline, and choline phosphate in the quantum mechanical approach. J_{HN} and J_{HP} represent the ^{1}H−^{14}N and ^{1}H−^{31}P couplings, respectively.

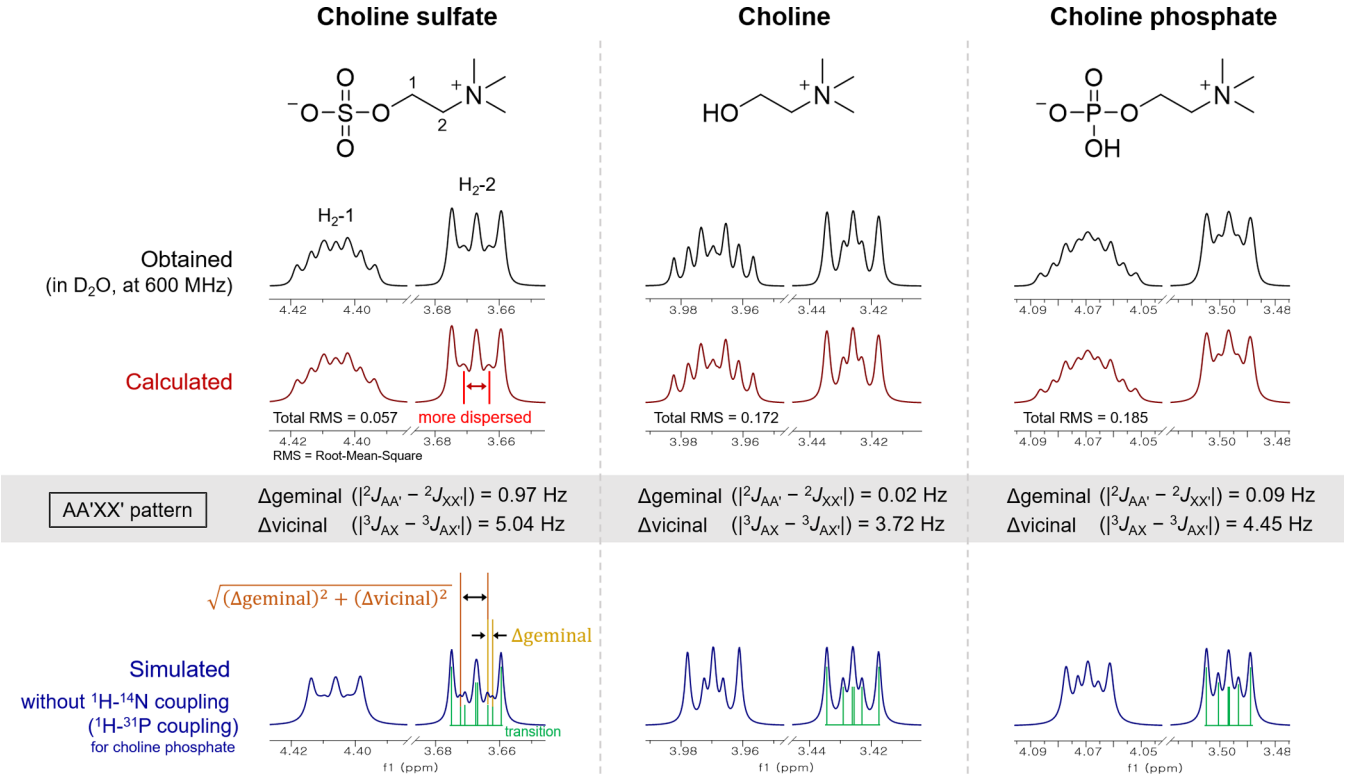

Figure 2. Comparison of H_2-1 and H_2-2 peak shapes according to differences in geminal and vicinal coupling constants in QM-HiFSA of choline sulfate, choline, and choline phosphate. The spectral simulations were performed excluding the ^{1}H−^{14}N and ^{1}H−^{31}P couplings to highlight the phenomenon.

and choline esters account for the distinct methylene proton resonance patterns. Accordingly, the complex peak patterns obtained in D_2O were previously analyzed to investigate their conformational properties in aqueous solution. The conformation in aqueous solution, rather than the conformation of solid crystals, was considered to describe the actual physiological functions.[20,23−27] The previous studies to elucidate an implicit association between the conformer population and magnitudes of two different vicinal coupling constants suggested that the "O−C−C−N$^+$" system predominantly exists in the *gauche* conformation in aqueous solution, as analyzed by the determination of crystal structures.[20,24,26] The electrostatic attraction between the positively charged quaternary nitrogen and electronegative oxygen can be attributed to the stabilization of the gauche conformation of choline and choline esters.[28]

As analyzed in the previous section, the two-bond heteronuclear coupling (i.e., $^2J_{HN}$ and $^2J_{HP}$) is small and thus only broadens the observed peak shape. On the other hand, the value of the three-bond heteronuclear coupling (i.e., $^3J_{HN}$ and $^3J_{HP}$) is large enough to cause additional peaks in the H_2-1 resonance pattern. In this regard, previous manual spectral analyses have interpreted the relatively simple H_2-2 pattern to obtain H-1/H-2 vicinal couplings.[20,24] However, recently, computer-assisted spectral analysis has allowed the determination of geminal and vicinal couplings in highly complex H_2-1 resonance patterns.[15,16] The QM-HiFSA in the present study yielded a complete analysis of the geminal ($^2J_{HH}$) and vicinal ^{1}H−^{1}H couplings ($^3J_{HH}$) of choline sulfate (Table 1): $^2J_{HH}$ = −13.81 Hz and $^3J_{HH}$ = 7.16 and 2.12 Hz, respectively. Optimized vicinal coupling values of choline and choline phosphate were also obtained (choline, $^3J_{HH}$ = 6.89 and 3.16 Hz; choline phosphate, $^3J_{HH}$ = 6.98 and 2.54 Hz), which were consistent with previously reported values[15,16] and also comparable to those of choline sulfate.

As described above, the complexity of the ^{1}H spin systems of choline and choline esters arises from the occurrence of non-first-order splitting, in addition to the presence of heteronuclear coupling. Given three stable staggered conformers (one *anti*- and two *gauche*-conformers), the AA′XX′ spin system exhibits first-order triplets when the three conformers are equally

https://doi.org/10.1021/acsomega.2c06092
ACS Omega 2022, 7, 42607−42612

dominant. However, conformational predominance results in magnetic non-equivalence between the chemically equivalent geminal protons (i.e., non-first-order effect).[29] In this context, the observation of the non-first-order spin systems indicated the presence of conformational predominance in the "O−C−C−N^+" system of choline and choline esters. Moreover, the magnitude of the two different vicinal couplings (∼7 and ∼2 Hz, respectively) in QM-HiFSA is the rationale for the predominance of *gauche* conformation,[29] which is consistent with the interpretation of previous studies.[20,24,26]

3.3. Further Complexity in the H_2-2 Resonance Pattern of Choline Sulfate. A closer examination revealed a subtle difference in the H_2-2 resonance pattern of choline sulfate compared to those of choline and choline phosphate (Figure 2, the equations in the figure have been adopted from the literature[30]). To further investigate the peak pattern differences associated with geminal and vicinal couplings, spectral simulations, excluding the heteronuclear coupling, were performed. From a constructive perspective on the pattern appearance, the transitions contributing to the middle line of the first-order triplet were offset from the center by the difference between the two vicinal couplings [Δvicinal ($|^3J_{AX} - {}^3J_{AX'}|$)].[30] The dispersion degree was apparently observed to be correlated with the size of Δvicinal, which was of the order "choline sulfate (5.04 Hz) > choline phosphate (4.45 Hz) > choline (3.72 Hz)".

Moreover, the spectral simulation exposed additional lines of the H_2-2 resonance pattern of choline sulfate, which were concealed under the signal broadening effects of the $^1H-^{14}N$ coupling. It was determined that the line shape observed only in choline sulfate is a consequence of the substantial difference between the two geminal couplings [Δgeminal ($|^2J_{AA'} - {}^2J_{XX'}|$), choline sulfate 0.97 Hz; choline, 0.02 Hz; choline phosphate, 0.09 Hz]. As geminal and vicinal couplings were significantly affected by conformational changes due to differences in structural subcomponents,[14,30] the presence of sulfate or phosphate units in the choline moiety was considered a factor for the different sizes of Δgeminal and Δvicinal.

3.4. Perspectives and Applications. The strength of QM-HiFSA profile development lies in its wide range of applications. First of all, the complete documentation of the spectral parameters of the QM-HiFSA profile is adequate enough to significantly contribute to the ^1H NMR-driven dereplication and metabolomic identification. A database of complete NMR profiles makes QM-HiFSA a powerful tool for rapid structure dereplication of single or multiple molecules from mixtures. Moreover, the high precision of the QM-HiFSA profiles (δ and J values at levels of 0.1 ppb and 10 mHz, respectively) allows for unambiguous structure identification and can further provide descriptions of structurally similar molecules.[13] Regarding the quantitative capability of NMR, QM-HiFSA enhances spectral deconvolution, especially for multi-target quantification of mixtures. Non-QM deconvolution methods (e.g., global spectral deconvolution peak fitting) still avoid highly overlapping resonances and fail to deconvolute accurately when non-first-order situations exist. In order to perform QM-qNMR, the development of the QM-HiFSA profile of the target molecule must be preceded.[10]

The development of the QM-HiFSA profile is also expected to facilitate the utilization of low-field benchtop NMR. The compact benchtop NMR has significant economic and environmental benefits. In addition, recently, it has been reintroduced for various purposes such as quality control of natural products.[31] On one hand, however, the less resolved spectra of the low-field NMR limit its usefulness. It is noteworthy that QM-HiFSA profiles generated using experimental data at high magnetic fields can be used to simulate spectra obtained from the low-field NMR. That is, the QM-based analysis using the QM-HiFSA profile with full assignments is viable even when using the benchtop NMR for experimental data acquisition.[8,11,32] In the context described above, this study presents for the first time a fully characterized QM-HiFSA profile of choline sulfate, with anticipation of future contributions to QM-based qualitative and quantitative studies independent of magnetic field strength.

The generated QM-HiFSA profile can also provide prior knowledge of spectral parameters for new QM-HiFSA studies of structurally similar molecules.[11] The QM-HiFSA profiles of choline and choline esters developed in the present study include a complete interpretation of the heteronuclear coupling in the presence of the ^{14}N nucleus located in the highly symmetrical environment. The calculated J_{HN} values of choline and choline esters can be applied as starting values for the iterative optimization of NMR parameters of biologically important tetraalkylammonium compounds such as carnitine and carnitine esters.[33,34]

4. CONCLUSIONS

The iterative optimization in the present study fully determined the spectral parameters, including the chemical shift, coupling constant, and line width, in the ^1H NMR spectrum of choline sulfate. Heteronuclear coupling and non-first-order splitting were analyzed to be the two major factors contributing to the complexity of the ^1H spin systems. First, the computational analysis enabled the complete determination of the $^1H-^{14}N$ heteronuclear coupling, including the small two-bond coupling, which was a remaining issue in conventional manual spectral analysis. Second, the QM-HiFSA process fully interpreted the non-first-order spin systems, indicating the presence of conformational predominance in the "O−C−C−N^+" system of choline sulfate, as reported for choline and choline phosphate. Spectral simulations, excluding heteronuclear coupling effects, distinctly demonstrated the difference in the line shapes of choline sulfate compared to those of choline and choline phosphate. Choline sulfate showed additional lines, along with a relatively large dispersion of transitions. The absolute sizes of Δgeminal and Δvicinal were analyzed to determine the differences in line shapes. Collectively, computer-assisted spectral analysis based on quantum mechanics efficiently addressed the challenges in the conventional manual analysis of ^1H spin complexity, allowing access to detailed spectral and structural information of choline sulfate.

■ ASSOCIATED CONTENT

Supporting Information

The Supporting Information is available free of charge at https://pubs.acs.org/doi/10.1021/acsomega.2c06092.

The full QM-HiFSA fingerprints and profiles in the ChemAdder parameter (.pmr) file format of choline sulfate, choline, and choline phosphate (PDF)

NMR raw data for choline sulfate acquired in D_2O at 600 MHz (ZIP)

https://doi.org/10.1021/acsomega.2c06092
ACS Omega 2022, 7, 42607−42612

AUTHOR INFORMATION

Corresponding Author

Joo-Won Nam − *College of Pharmacy, Yeungnam University, Gyeongsan-si, Gyeongsangbuk-do 38541, South Korea;* orcid.org/0000-0001-5502-0736; Email: jwnam@yu.ac.kr

Author

Yun-Seo Kil − *College of Pharmacy, Yeungnam University, Gyeongsan-si, Gyeongsangbuk-do 38541, South Korea*

Complete contact information is available at: https://pubs.acs.org/10.1021/acsomega.2c06092

Author Contributions

All authors have approved the final version of the manuscript.

Notes

The authors declare no competing financial interest.

ACKNOWLEDGMENTS

This research was supported by the Brain Pool program (NRF-2019H1D3A1A01102673) funded by the Ministry of Science and ICT and the Basic Science Research Program funded by the Ministry of Education (NRF-2022R1A2C1009496), through the National Research Foundation of Korea (NRF). The authors are grateful to P. Laatikainen (Spin Discoveries, Finland) for his valuable technical support in computational NMR analysis.

REFERENCES

(1) Phillips, M. M. Analytical approaches to determination of total choline in foods and dietary supplements. *Anal. Bioanal. Chem.* **2012**, *403*, 2103−2112.

(2) Kil, Y.-S.; Han, A.-R.; Hong, M.-J.; Kim, J.-B.; Park, P.-H.; Choi, H.; Nam, J.-W. ^{1}H NMR-based chemometrics to gain insights into the bran of radiation-induced colored wheat mutant. *Front. Nutr.* **2022**, *8*, 806744.

(3) Nissen, P.; Benson, A. A. Choline sulfate in higher plants. *Science* **1961**, *134*, 1759.

(4) Nissen, P.; Benson, A. A. Active transport of choline sulfate by barley roots. *Plant Physiol.* **1964**, *39*, 586−589.

(5) Spencer, B.; Harada, T. Role of choline sulfate in the sulfur metabolism of fungi. *Biochem. J.* **1960**, *77*, 305.

(6) Fitzgerald, J. W.; Luschinski, P. C. Further studies on the formation of choline sulfate by bacteria. *Can. J. Microbiol.* **1977**, *23*, 483.

(7) Napolitano, J. G.; Lankin, D. C.; Graf, T. N.; Friesen, J. B.; Chen, S.-N.; McAlpine, J. B.; Oberlies, N. H.; Pauli, G. F. HiFSA fingerprinting applied to isomers with near-identical NMR spectra: The silybin/isosilybin case. *J. Org. Chem.* **2013**, *78*, 2827−2839.

(8) Napolitano, J. G.; Lankin, D. C.; McAlpine, J. B.; Niemitz, M.; Korhonen, S.-P.; Chen, S.-N.; Pauli, G. F. Proton fingerprints portray molecular structures: Enhanced description of the ^{1}H NMR spectra of small molecules. *J. Org. Chem.* **2013**, *78*, 9963−9968.

(9) Napolitano, J. G.; Gödecke, T.; Lankin, D. C.; Jaki, B. U.; McAlpine, J. B.; Chen, S.-N.; Pauli, G. F. Orthogonal analytical methods for botanical standardization: Determination of green tea catechins by qNMR and LC-MS/MS. *J. Pharm. Biomed. Anal.* **2014**, *93*, 59−67.

(10) Phansalkar, R. S.; Simmler, C.; Bisson, J.; Chen, S.-N.; Lankin, D. C.; McAlpine, J. B.; Niemitz, M.; Pauli, G. F. Evolution of quantitative measures in NMR: Quantum mechanical qHNMR advances chemical standardization of a red clover (*Trifolium pratense*) extract. *J. Nat. Prod.* **2017**, *80*, 634−647.

(11) Achanta, P. S.; Jaki, B. U.; McAlpine, J. B.; Friesen, J. B.; Niemitz, M.; Chen, S.-N.; Pauli, G. F. Quantum mechanical NMR full spin analysis in pharmaceutical identity testing and quality control. *J. Pharm. Biomed. Anal.* **2021**, *192*, 113601.

(12) Pauli, G. F.; Ray, G. J.; Bzhelyansky, A.; Jaki, B. U.; Corbett, C.; Szabo, C.; Steinbeck, C.; Sørensen, D.; Jeannerat, D.; Ferreira, D.; et al. Consistent terminology for advancement of NMR spectroscopy. *Pharm. Forum.* **2022**, *48*, 1−8.

(13) Pauli, G. F.; Chen, S.-N.; Lankin, D. C.; Bisson, J.; Case, R. J.; Chadwick, L. R.; Gödecke, T.; Inui, T.; Krunic, A.; Jaki, B. U.; et al. Essential parameters for structural analysis and dereplication by ^{1}H NMR spectroscopy. *J. Nat. Prod.* **2014**, *77*, 1473−1487.

(14) Kil, Y.-S.; Baral, A.; Jeong, B.-S.; Laatikainen, P.; Liu, Y.; Han, A.-R.; Hong, M.-J.; Kim, J.-B.; Choi, H.; Park, P.-H.; et al. Combining NMR and MS to describe pyrrole-2-carbaldehydes in wheat bran of radiation. *J. Agric. Food Chem.* **2022**, *70*, 13002−13014.

(15) Achanta, P. S.; Niemitz, M.; Friesen, J. B.; Tadjimukhamedov, F. K.; Bzhelyansky, A.; Giancaspro, G. I.; Chen, S.-N.; Pauli, G. F. Pharmaceutical analysis by NMR can accommodate strict impurity thresholds: The case of choline. *J. Pharm. Biomed. Anal.* **2022**, *214*, 114709.

(16) Govindaraju, V.; Young, K.; Maudsley, A. A. Proton NMR chemical shifts and coupling constants for brain metabolites. *NMR Biomed.* **2000**, *13*, 129−153.

(17) Murari, R.; Baumann, W. J. Quadrupolar carbon-13-nitrogen-14 couplings and nitrogen-14 relaxations in aggregated and nonaggregated choline phospholipids. *J. Am. Chem. Soc.* **1981**, *103*, 1238.

(18) London, R. E.; Walker, T. E.; Wilson, D. M.; Matwiyoff, N. A. Application of doubly decoupled carbon-13 {proton, nitrogen-14}-NMR spectroscopy to studies of the conformation and dynamics of the choline headgroup of phospholipids. *Chem. Phys. Lipids* **1979**, *25*, 7−14.

(19) Kaech, A.; Hofer, M.; Rentsch, D.; Schnider, C.; Egli, T. Metabolites and dead-end products from the microbial oxidation of quaternary ammonium alcohols. *Biodegradation* **2005**, *16*, 461−473.

(20) Dufourcq, J.; Lussan, C. Conformations of the phosphatidylcholine and phosphatidylethanolamine polar groups determined by NMR spectroscopy. *FEBS Lett.* **1972**, *26*, 35.

(21) Basti, M. M.; LaPlanche, L. A. ^{1}H-, ^{13}C- and ^{31}P-NMR studies of dioctanoylphosphatidylcholine and dioctanoylthiophosphatidylcholine. *Chem. Phys. Lipids* **1990**, *54*, 99−113.

(22) Haapaniemi, E. Complete ^{1}H, ^{13}C{^{1}H}, and ^{31}P NMR spectral parameters of some pyrophosphates. *Magn. Reson. Chem.* **2017**, *55*, 804−812.

(23) Senko, M. E.; Templeton, D. H. Unit cells of choline halides and structure of choline chloride. *Acta Crystallogr.* **1960**, *13*, 281.

(24) Culvenor, C. C. J.; Ham, N. S. Proton magnetic resonance spectrum and conformation of acetylcholine. *Chem. Commun.* **1966**, 537.

(25) Post, M. L. Choline O-sulphate. *Acta Crystallogr., Sect. B: Struct. Sci., Cryst. Eng. Mater.* **1978**, *34*, 1741.

(26) Hauser, H.; Guyer, W.; Pascher, I.; Skrabal, P.; Sundell, S. Polar group conformation of phosphatidylcholine. Effect of solvent and aggregation. *Biochemistry* **1980**, *19*, 366.

(27) Hauser, H.; Guyer, W.; Spiess, M.; Pascher, I.; Sundell, S. The polar group conformation of a lysophosphatidylcholine analogue in solution. A high-resolution nuclear magnetic resonance study. *J. Mol. Biol.* **1980**, *137*, 265.

(28) Sundaralingam, M. Conformational relations between the OCCN+ system of phospholipids and substrates on muscarinic and cholinergic systems. *Nature* **1968**, *217*, 35.

(29) Hans Reich's Collection. NMR Spectroscopy. https://organicchemistrydata.org/hansreich/resources/nmr (accessed Nov 10, 2022).

(30) Stevenson, P. J. Second-order NMR spectra at high field of common organic functional groups. *Org. Biomol. Chem.* **2011**, *9*, 2078−2084.

(31) Beek, T. A. Low-field benchtop NMR spectroscopy: status and prospects in natural product analysis. *Phytochem. Anal.* **2021**, *32*, 24−37.

(32) Napolitano, J. G.; Lankin, D. C.; Chen, S.-N.; Pauli, G. F. Complete ^{1}H NMR spectral analysis of ten chemical markers of *Ginkgo biloba*. *Magn. Reson. Chem.* **2012**, *50*, 569−575.
(33) Virmani, A.; Binienda, Z. Role of carnitine esters in brain neuropathology. *Mol. Aspects Med.* **2004**, *25*, 533−549.
(34) Flanagan, J. L.; Simmons, P. A.; Vehige, J.; Willcox, M. D. P.; Garrett, Q. Role of carnitine in disease. *Nutr. Metab.* **2010**, *7*, 30.

https://doi.org/10.1021/acsomega.2c06092
ACS Omega 2022, 7, 42607−42612